PROCEEDINGS OF SCIENCE

CP violation in charm with LHCb

Martha Hilton* **On behalf of the LHCb Collaboration**
University of Manchester
E-mail: martha.hilton@cern.ch

Measurements of charge-parity (*CP*) violation and mixing in charm allow tests of the Standard Model and can potentially probe physics beyond the Standard Model. The violation of *CP* symmetry has been well established in the kaon and beauty sectors and was first observed in charm at the LHCb experiment in 2019. The LHCb detector is specifically designed for measurements of *CP* violation and mixing and has provided some of the most precise measurements to date. The large production cross-section of charm hadrons and the versatility of the LHCb trigger allow for tight control of systematic uncertainties and therefore precise measurements of *CP* asymmetries. The first observation of *CP* violation in charm is presented, as well as searches for direct *CP* violation in two-body decays, and a measurement of the difference in mass eigenstates of the neutral charm meson.

7th Annual Conference on Large Hadron Collider Physics - LHCP2019
20-25 May, 2019
Puebla, Mexico

*Speaker.

© Copyright owned by the author(s) under the terms of the Creative Commons
Attribution-NonCommercial-NoDerivatives 4.0 International License (CC BY-NC-ND 4.0).

PoS(LHCP2019)203

1. Introduction

In the Standard Model (SM) of particle physics, *CP* violation is introduced through an irreducible complex phase in the Cabibbo-Kobayashi-Maskawa (CKM) mixing matrix [1]. However the amount of *CP* violation allowed in the SM is too small to account for the matter-antimatter asymmetry observed in the universe. Measurements of *CP* violation have been performed in the kaon and beauty sectors [2, 3] but until 2019 *CP* violation had not been discovered in charm [4]. Measurements of *CP* violation in charm are complimentary to those in kaon and beauty and provide a unique opportunity to measure *CP* violation in particles containing only up-type quarks. Theoretical predictions of *CP* violation in the charm sector are $\mathcal{O}(10^{-3}-10^{-4})$ [5], but due to low-energy strong interactions they are difficult to compute reliably. Contributions of physics beyond the SM may alter the size of *CP* violation in charm, therefore making searches for *CP* asymmetries a potentially sensitive probe of new physics.

Mixing between a neutral meson and its antiparticle occurs because the mass eigenstates of neural mesons are linear combinations of the flavour eigenstates. New virtual particles may contribute in the amplitude, enhancing the oscillation rate, making flavour oscillations potentially sensitive to new physics. The mass eigenstates of a neutral charm meson are given by:

$$|D_{1,2}\rangle \equiv p\,|D^0\rangle \pm q\,|\overline{D}^0\rangle\,, \tag{1.1}$$

where p and q are complex parameters. The time-dependent oscillations are characterised by the mixing parameters:

$$x \equiv \frac{(m_1-m_2)}{\Gamma} \qquad ,y \equiv \frac{(\Gamma_1-\Gamma_2)}{2\Gamma}, \tag{1.2}$$

where $m_{1,2}$ and $\Gamma_{1,2}$ are the masses and widths of the mass eigenstates $D_{1,2}$ and $\Gamma = (\Gamma_1+\Gamma_2)/2$.

There are three different types of *CP* violation in the SM. Direct *CP* violation in decay occurs when:

$$\Gamma(D^0 \to f) \neq \Gamma(\overline{D}^0 \to \overline{f}); \tag{1.3}$$

indirect *CP* violation in mixing occurs when:

$$\Gamma(D^0 \to \overline{D}^0) \neq \Gamma(\overline{D}^0 \to D^0); \tag{1.4}$$

and *CP* violation in the interference between mixing and decay occurs when:

$$\Gamma(D^0 \to \overline{D}^0 \to f,t) \neq \Gamma(\overline{D}^0 \to D^0 \to f,t). \tag{1.5}$$

The LHCb detector [6] is a forward detector specifically designed for the study of b and c hadrons. The large cross-section of charm at the LHC and the dedicated LHCb trigger allows measurements of *CP* violation in charm with previously unreachable precision [7] [8]. The LHCb turbo stream allows candidates to be reconstructed online in the trigger increasing the data output rate [9]. The first observation of *CP* violation in the charm sector will be presented in Section 2. The measurement of the mass difference between neutral charm eigenstates is presented in Section 3, a measurement of direct *CP* asymmetries is presented in Section 4 and a measurement of the *CP* violation parameter A_Γ is presented in Section 5.

PoS(LHCP2019)203

2. Observation of *CP* violation in charm decays

The time-integrated *CP* asymmetry, A_{CP}, in the decay of neutral D mesons to some final state f is given by:

$$A_{CP}(f) = \frac{\Gamma(D^0 \to f) - \Gamma(\overline{D}^0 \to f)}{\Gamma(D^0 \to f) + \Gamma(\overline{D}^0 \to f)}. \tag{2.1}$$

The difference in time-integrated asymmetries in the $D^0 \to K^+K^-$ and $D^0 \to \pi^+\pi^-$ channels is given by:

$$\begin{aligned} \Delta A_{CP} &\equiv A_{CP}(K^+K^-) - A_{CP}(\pi^+\pi^-) \\ &\approx \Delta a_{CP}^{dir} - \frac{\Delta\langle t\rangle}{\tau(D^0)} A_\Gamma, \end{aligned} \tag{2.2}$$

where $\Delta a_{CP}^{dir} \equiv a_{CP}^{dir}(K^+K^-) - a_{CP}^{dir}(\pi^+\pi^-)$ and $\Delta\langle t\rangle = \langle t\rangle_{KK} - \langle t\rangle_{\pi\pi}$. A_Γ is the asymmetry between the $D^0 \to f$ and $\overline{D}^0 \to f$ effective decay widths. This analysis uses data collected during Run 2 of the LHC, corresponding to an integrated luminosity of 5.9 fb^{-1}. The D^0 mesons analysed are produced either from prompt $D^{*+} \to D^0\pi^+$ decays, which come directly from the pp collision, or from the inclusive semileptonic B meson decay $B \to \overline{D}^0\mu^+X$. The initial flavour of the neutral D meson is tagged by the charge of the pion in the prompt sample and by the charge of the muon in the semileptonic sample.

The raw asymmetries are given by:

$$A_{raw}(f) = \frac{N(D^0 \to f) - N(\overline{D}^0 \to f)}{N(D^0 \to f) + N(\overline{D}^0 \to f)}, \tag{2.3}$$

where N is the number of reconstructed signal decays after preselection. This can be approximated as:

$$\begin{aligned} A_{raw}^{\pi-\text{tagged}}(f) &\approx A_{CP}(f) + A_D(\pi) + A_P(D^*) \\ A_{raw}^{\mu-\text{tagged}}(f) &\approx A_{CP}(f) + A_D(\mu) + A_P(B), \end{aligned} \tag{2.4}$$

where A_D and A_P are the detection and production asymmetries, respectively. The production and detection asymmetries are independent of the final state f and largely cancel, resulting in:

$$\Delta A_{CP} = A_{raw}(K^+K^-) - A_{raw}(\pi^+\pi^-), \tag{2.5}$$

and making the quantity ΔA_{CP} largely insensitive to systematic uncertainties.

The data used in this analysis is selected in several steps including: requirements on the hardware trigger decision, particle identification requirements and removal of multiple candidates. For the μ-tagged sample, data is further filtered by the use of a multivariate classifier. For the π-tagged sample, a requirement is used to suppress background from D^0 mesons from semileptonic decays of b hadrons.

Large detection asymmetries can occur in certain kinematic regions of the tagging muon or pion. Low-momentum charged particles may be deflected out of the detector whereas particles of the opposite charge may remain in acceptance. These events are therefore removed from the

PoS(LHCP2019)203

analysis by fiducial requirements. As the production and detection asymmetries are dependent on the kinematics of the final state particles, the cancellation may be incomplete if the kinematics of the K^+K^- and $\pi^+\pi^-$ decay modes differ; this is accounted for with a weighting procedure. This weighting procedure leads to a small variation in ΔA_{CP} of below 10^{-4} and is accounted for by a systematic uncertainty.

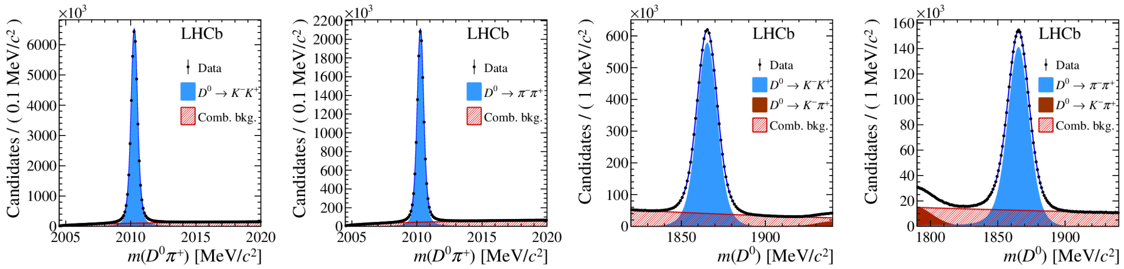

Figure 1: Mass distributions for selected π-tagged and μ-tagged candidates for K^+K^- and $\pi^+\pi^-$ final states of D^0 meson decays with fit projections.

The raw asymmetries are determined by means of simultaneous fits to the D^{*+} and D^{*-} mass distributions for the π-tagged sample and the D^0 and $\overline{D}^0$ mass distributions for the μ-tagged sample. For the π-tagged sample, the signal is modelled by the sum of three Gaussian functions and a Johnson S_U function [10], while the background is described by an empirical function. For the μ-tagged sample the signal is modeled by the sum of two Gaussian functions convoluted with a truncated power-law function which accounts for final-state photon radiation effects. The background is described by an exponential function; a small contribution from $D^0 \to K^-\pi^+$ decays is modeled by the tail of a Gaussian function. The fits can be seen in Figure 1; the signal yields are 44 M (9 M) $D^0 \to K^+K^-$ reconstructed events and 14 M (3 M) $D^0 \to \pi^+\pi^-$ events in the prompt (semileptonic) samples.

Several sources of systematic uncertainties are considered independently for the π-tagged and μ-tagged samples. For the π-tagged sample, the dominant source of systematic uncertainty is related to the knowledge of the signal and background mass models; this is evaluated by generating pseudoexperiments according to the baseline fit model and fitting alternative models to the data. In the case of the μ-tagged sample, the dominant systematic uncertainty is due to the possibility that the D^0 flavour is not tagged correctly due to misreconstruction; this is evaluated using a control sample of $D^0 \to K^-\pi^+$ decays, as *CP* violation in this decay is expected to be significantly below the current experimental precision. Other sources of systematic uncertainty include: knoweldge of the weights used in the kinematic reweighting procedure; contamination from D^0 mesons from semileptonic decays in the prompt sample, evaluated by performing a fit to the D^0 impact parameter.

The results for the difference in time-integrated *CP* asymmetries of $D^0 \to K^+K^-$ and $D^0 \to \pi^+\pi^-$ decays are:

$$\begin{aligned} \Delta A_{CP}^{\pi-\text{tagged}} &= [-18.2 \pm 3.2(\text{stat}) \pm 0.9(\text{syst})] \times 10^{-4} \\ \Delta A_{CP}^{\mu-\text{tagged}} &= [-9 \pm 8(\text{stat}) \pm 5(\text{syst})] \times 10^{-4}. \end{aligned} \tag{2.6}$$

Both measurements are in good agreement with the world average and previous LHCb re-

PoS(LHCP2019)203

sults [11, 12]. By combining with previous LHCb results, the following value for ΔA_{CP} is obtained:

$$\Delta A_{CP} = (-15.4 \pm 2.9) \times 10^{-4}. \tag{2.7}$$

This result deviates from zero with a significance of 5.3 standard deviations and corresponds to the first observation of *CP* violation in the decay of charm hadrons. This result is consistent with SM predictions. The current world averages and comparison with the no *CP* violation hypothesis are shown in Figure 2.

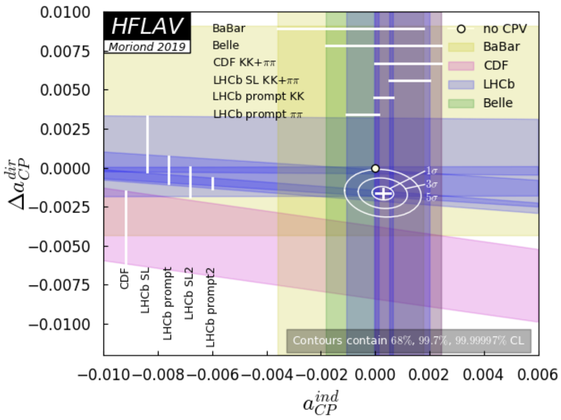

Figure 2: World averages of the direct and indirect *CP* violation parameters.

3. Measurement of the mass difference between neutral charm-meson eigenstates

The time-dependent amplitude of the $D^0 \to K_s^0\pi^+\pi^-$ decay is given by:

$$\begin{aligned}|\mathcal{A}_f(t)|^2 = \frac{1}{2}e^{-\Gamma t}\Bigg[&\left(|\mathcal{A}_f|^2 - \left|\frac{q}{p}\overline{\mathcal{A}}_f\right|^2\right) cos(x\Gamma t) - 2\,\mathrm{Im}\left\{\mathcal{A}_f\overline{\mathcal{A}}_f^*\left(\frac{q}{p}^*\right)\right\} sin(x\Gamma t)\\ &+ \left(|\mathcal{A}_f|^2 + \left|\frac{q}{p}\overline{\mathcal{A}}_f\right|^2\right) cosh(y\Gamma t) - 2\,\mathrm{Re}\left\{\mathcal{A}_f\overline{\mathcal{A}}_f^*\left(\frac{q}{p}^*\right)\right\} sinh(y\Gamma t)\Bigg].\end{aligned} \tag{3.1}$$

The self-conjugate $D^0 \to K_s^0\pi^+\pi^-$ decay offers direct experimental access to the mixing parameters x and y. The mixing parameters can be extracted from a time-dependent fit to the Dalitz plot of this decay. This approach is challenging, due mainly to the modelling of the three-body decay dynamics, calculation of detector efficiencies across the Dalitz plane and accurate determination of the decay-time acceptance effects. This analysis uses the model-independent bin-flip approach, which is optimised for the parameter x [13]. This method relies on ratios between decays reconstructed in similar phase-space and decay-time conditions, avoiding the need for accurate modeling of the efficiency variation across phase-space and decay time.

The dynamics of the three-body $D^0 \to K_s^0\pi^+\pi^-$ decay can be described by the Dalitz formalism where $m_\pm^2 \equiv m^2(K_S^0\pi^\pm)$ for D^0 decays and $m_\pm^2 \equiv m^2(K_S^0\pi^\mp)$ for $\overline{D}^0$. The Dalitz plot is divided into symmetric bins of approximately constant strong-phase difference, indexed $\pm b$ (shown in Figure 3); the data is further split into bins of decay time, indexed j. For each bin the ratios R_{bj}^+ and

PoS(LHCP2019)203

R^{-}_{bj} of initially produced D^0 ($\overline{D}^0$) mesons in symmetric bins $-b$ and $+b$ is measured:

$$R^{\pm}_{bj} \approx \frac{r_b + \frac{1}{4} r_b \left\langle t^2 \right\rangle_j Re(z_{cp}^2 - \Delta z^2) + \frac{1}{4} \left\langle t^2 \right\rangle_j |z_{cp} \pm \Delta z|^2 + \sqrt{r_b} \left\langle t \right\rangle_j Re[X_b^*(z_{CP} \pm \Delta z)]}{1 + \frac{1}{4} \left\langle t^2 \right\rangle_j Re(z_{CP}^2 - \Delta z^2) + r_b \frac{1}{4} \left\langle t^2 \right\rangle_j |z_{CP} \pm \Delta z|^2 + \sqrt{r_b} \left\langle t \right\rangle_j Re[X_b(z_{CP} \pm \Delta z)]}, \tag{3.2}$$

where $\langle t \rangle_j$ is the average decay time of unmixed decays in bin j, r_b is the ratio of signal yields in symmetric Dalitz bins $\pm b$ at $t = 0$, X_b is the average strong phase difference in each bin determined from external inputs. The parameters z_{CP} and Δz are obtained from a fit to $R^{\pm}_{bj}$ ratios in decay time. The mixing and *CP* violation parameters can be derived from the fit parameters by $z_{CP} \pm \Delta z \equiv -(q/p)^{\pm 1}(y + ix)$.

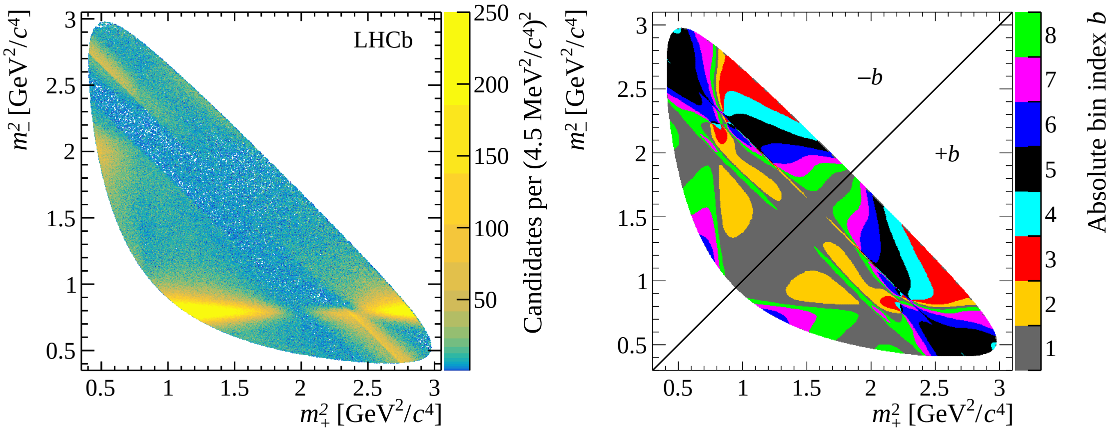

Figure 3: Dalitz plot distribution of background subtracted $D^0 \to K^0_S \pi^+ \pi^-$ decays (left) and binning scheme (right).

This analysis uses *pp* collision data collected during the Run 1 data-taking period in 2011-2012, corresponding to an integrated luminosity of 3 fb^{-1}. Neutral D mesons from prompt $D^{*+} \to D^0 \pi^+$ and semileptonic $B \to D^0 \mu X$ decays are used. Selection requirements include criteria on the momenta and displacement from the primary vertex, particle-identification information and invariant mass of the D^{*+} decay products for the prompt sample. The prompt and semileptonic data samples correspond to 1.3 and 1.0 million candidates, respectively.

Selection requirements on the kinematics of the D^0 decay products introduce efficiency variations that are correlated between $m^2(\pi^+\pi^-)$ and decay time, potentially biasing the results. A per-candidate event weight of the inverse of the efficiency is applied to each candidate, where the efficiency is determined from background subtracted $(m^2(\pi^+\pi^-), t)$ distribution in data. The correction is symmetric in m^+ and m^-. The signal yields in each bin are determined by fits to the $\Delta m \equiv m(D^{*+}) - m(D^0)$ distribution for the prompt sample and the $m(D^0)$ distribution for the semileptonic sample. The mixing and *CP* violation parameters are determined from a least-squares fit to the ratios of yields in the symmetric bins in decay time, shown in Figure 4.

PoS(LHCP2019)203

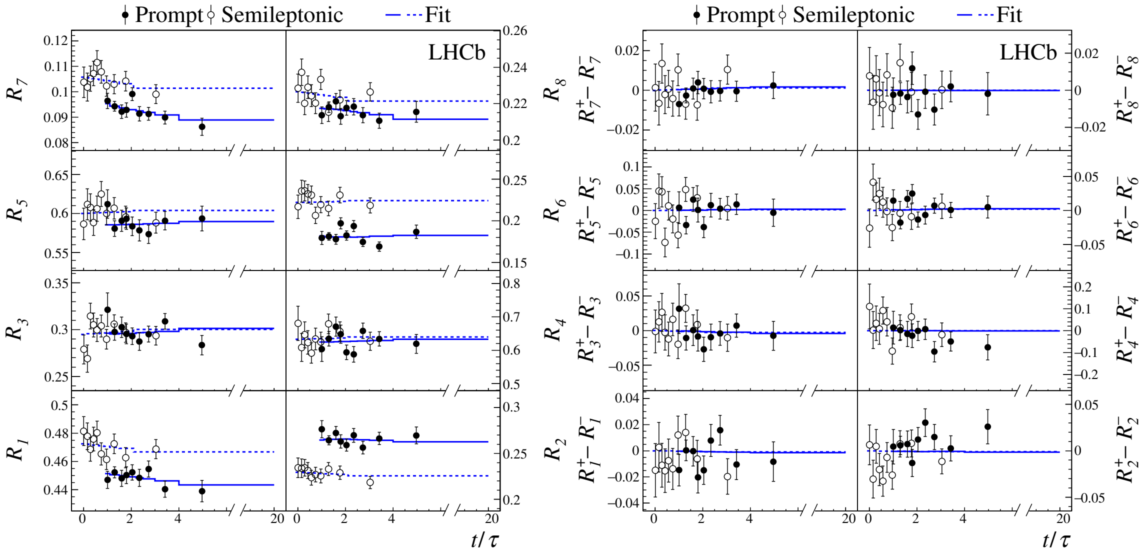

Figure 4: Ratios (left) and differences (right) of D^0 and $\overline{D}^0$ yields as a function of t/τ in each Dalitz bin and fit projections for prompt (closed points and solid line) and semileptonic (open points and dashed line) samples.

The results of the mixing and *CP* violation parameters are:

$$\begin{aligned} x_{CP} &\equiv (2.7 \pm 1.6 \pm 0.4) \times 10^{-3} \\ y_{CP} &\equiv (7.4 \pm 3.6 \pm 1.1) \times 10^{-3} \\ \Delta x &\equiv (-0.53 \pm 0.70 \pm 0.22) \times 10^{-3} \\ \Delta y &\equiv (0.6 \pm 1.6 \pm 0.3) \times 10^{-3}, \end{aligned} \tag{3.3}$$

where the uncertainties are statistical and systematic respectively. The mixing and *CP* violation parameters x, y, $|q/p|$ and ϕ can be derived from x_{CP}, y_{CP}, Δx and Δy. The results are consistent with the world average and with the *CP* symmetry hypothesis. This result is the most precise determination of x from a single experiment. The dominant systematic uncertainty on x_{CP} is the contamination from secondary D^{*+} decays in the prompt sample and the contamination of genuine D^0 mesons associated with random muons in the semileptonic sample. The dominant systematic uncertainty on the parameter y_{CP} is due to decay time and $m^2_{\pm}$ resolutions and efficiency variations. The impact of the results on the world average is shown in Figure 5. The new world average gives $x > 0$ with a significance of greater than 3 standard deviations which corresponds to the first evidence of a non-zero mass difference between the neutral charm eigenstates.

4. Search for *CP* violation in $\mathrm{D_s^+} \to \mathrm{K_s^0}\pi^+$, $\mathrm{D^+} \to \mathrm{K_s^0 K^+}$ and $\mathrm{D^+} \to \phi\pi^+$ decays

A promising area to search for *CP* violation are correlations between *CP* asymmetries in $SU(3)$ related decays. In these decays, *CP* violation can occur in the interference between loop and tree level processes in $c \to d\bar{d}u$ and $c \to s\bar{s}u$ transitions. Contributions from beyond the SM physics can potentially enhance the size of *CP* violation in these decays [5].

PoS(LHCP2019)203

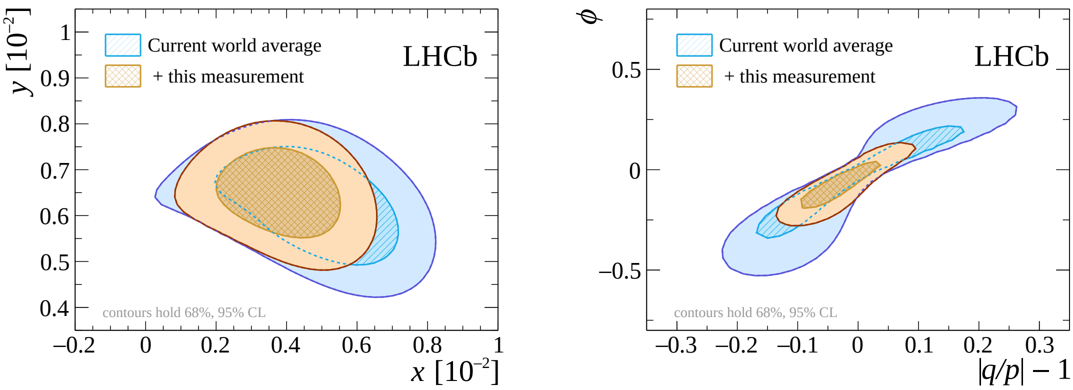

Figure 5: Impact on this result on the current world averages for the mixing parameters x and y (left) and CP violation parameters $|q/p|$ and ϕ (right).

A search for CP violation in the Cabibbo-suppressed $D_s^+ \to K_s^0\pi^+$, $D^+ \to K_s^0K^+$ and $D^+ \to \phi\pi^+$ decays was performed with a partial Run 2 dataset corresponding to 3.8 fb^{-1} [14]. The raw asymmetry is defined as:

$$A_{raw}^{D_{(s)}^+ \to f^+} \approx A_{CP}^{D_{(s)}^+ \to f^+} + A_P^{D_{(s)}^+} + A_D^{f^+}, \tag{4.1}$$

where $A_P^{D_{(s)}^+}$ and $A_D^{f^+}$ are the production and detection asymmetries respectively and f is the final state $K_s^0\pi^+$, $K_s^0K^+$ or $\phi\pi^+$. The detection and production asymmetries are cancelled using Cabibbo-favoured decays, for which the CP asymmetries are expected to be negligible compared to the Cabibbo-suppressed modes. The final CP symmetries are then:

$$\begin{aligned}
A_{CP}^{D_s^+ \to K_s^0\pi^+} &\approx A_{raw}^{D_s^+ \to K_s^0\pi^+} - A_{raw}^{D_s^+ \to \phi\pi^+} \\
A_{CP}^{D^+ \to K_s^0K^+} &\approx A_{raw}^{D^+ \to K_s^0K^+} - A_{raw}^{D^+ \to K_s^0\pi^+} - A_{raw}^{D_s^+ \to K_s^0K^+} + A_{raw}^{D_s^+ \to \phi\pi^+} \\
A_{CP}^{D^+ \to \phi\pi^+} &\approx A_{raw}^{D^+ \to \phi\pi^+} - A_{raw}^{D^+ \to K_s^0\pi^+} .
\end{aligned} \tag{4.2}$$

The data is selected in several stages, including online and offline trigger requirements, particle identification requirements, kinematic vetos and fiducial requirements. An artificial neural network is used to further suppress background using kinematic quantities of the particles. Since the detection and production asymmetries depend on the kinematics of the final state particles, a weighting procedure is necessary to ensure than the cancellation is complete. The ratio between background-subtracted signal and control sample distributions of certain kinematic variables are used to define per-candidate event weights.

The raw asymmetries of the decay modes of interest in Equation 4.2 are determined by simultaneous fits to the $D_{(s)}^+$ and $D_{(s)}^-$ invariant-mass distributions, seen in Figure 6. The approximate yields are: 600 k $D_s^+ \to K_S^0\pi^+$ decays, 5.1 M $D^+ \to K_S^0K^+$ decays and 53.3 M $D^+ \to \phi\pi^+$ decays. Several sources of systematic uncertainty are considered; the dominant systematic uncertainty is due to the signal and background fit models which is evaluated by pseudoexperiments where the data is fit with alternative models.

PoS(LHCP2019)203

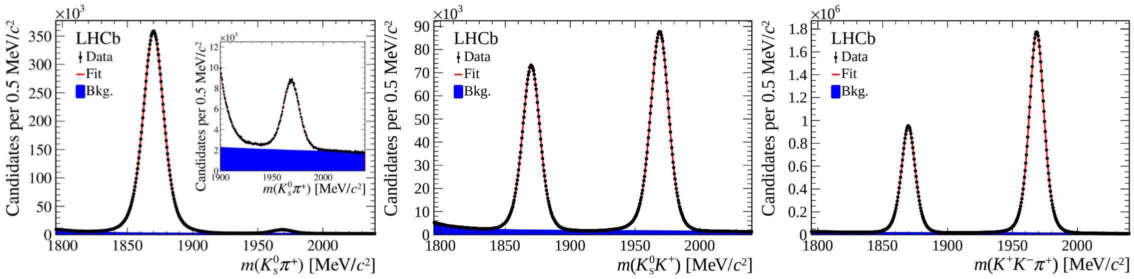

Figure 6: Invariant mass distributions of $D_s^+ \to K_s^0\pi^+$ (left), $D^+ \to K_s^0K^+$ (center), $D^+ \to \phi\pi^+$ (right) decays.

The final results of the CP asymmetries are as follows:

$$\begin{aligned} A_{CP}(D_s^+ \to K_s^0\pi^+) &= (1.3 \pm 1.9 \pm 0.5) \times 10^3 \\ A_{CP}(D^+ \to K_s^0K^+) &= (0.09 \pm 0.65 \pm 0.48) \times 10^3 \\ A_{CP}(D^+ \to \phi\pi^+) &= (0.05 \pm 0.42 \pm 0.29) \times 10^3, \end{aligned} \tag{4.3}$$

where the uncertainties are statistical and systematic respectively. This is the most precise determination of these quantities to date and the results are consistent with previous LHCb results [15, 16]. The results are consistent with the no CP violation hypothesis.

5. Search for time-dependent *CP* violation in $D^0 \to K^+K^-$ and $D^0 \to \pi^+\pi^-$ decays

A measurement of the CP violation parameter A_Γ can be performed with $D^0 \to K^+K^-$ and $D^0 \to \pi^+\pi^-$ decays [17]. The time-dependent asymmetry can be written as:

$$A_{CP}(f,t) \approx a_{CP}^{dir}(f) + a_{CP}^{ind}(f)(1+y_{CP})\frac{t}{\tau_{D^0}}, \tag{5.1}$$

where $a_{CP}^{dir}(f)$ and $a_{CP}^{indir}(f)$ are the direct and indirect CP asymmetries respectively. The quantity, $A_\Gamma(f)$ is the CP asymmetry in mixing or in the interference between mixing and decay where $A_\Gamma = -a_{CP}^{ind}$ when CP violation is small and y_{CP} can be neglected. The parameter A_Γ can be extracted from a linear fit to the time-dependent asymmetries in $D^0 \to K^+K^-$ and $D^0 \to \pi^+\pi^-$ decays.

This analysis uses a partial Run 2 dataset collected during 2015-2016, corresponding to an integrated luminosity of 1.9 fb^{-1}. This analysis uses D^0 mesons from prompt $D^{*+} \to D^0\pi^+$ decays, where the initial flavour is tagged by the charge of the pion. The time-dependent raw asymmetry is given by:

$$A_{raw}(f,t) \approx A_{CP}(f,t) + A_D(\pi^+) + A_P(D^{*+}), \tag{5.2}$$

where $A_D(\pi^+)$ and $A_P(D^{*+})$ are the detection and production asymmetries, respectively.

Large detection asymmetries are introduced as low-momentum charged particles may be deflected out of the detector whereas particles of the opposite charge may remain in the detector acceptance. In addition selection requirements can introduce correlations between the D^0 momentum and decay time, biasing the measurement of A_Γ. These detector-induced asymmetries are removed by weighting the three-dimensional momentum distributions of the D^0 candidates. This

PoS(LHCP2019)203

causes a dilution of the measured value of A_Γ which is accounted for with a scale factor. Contamination from D^0 mesons from secondary B meson decays is accounted for by fitting the impact parameter in the plane transverse to the beam (TIP) in decay-time bins. In order to measure A_Γ, the time-dependent asymmetry in primary decays obtained from the TIP distribution is fitted with a linear function.

Several sources of systematic uncertainty are investigated including: residual backgrounds under the D^0 mass peak, correlations between the background asymmetry and the values of the D^{*+} mass and choice of binning for the kinematic reweighting. The main source of systematic uncertainty is due to the knowledge of the contamination from secondary decays, evaluated by fitting the TIP distribution with different resolution functions and constraining the fraction of secondary decays to that obtained from simulation or from a sample of decays which combine the D^{*+} candidate with a muon.

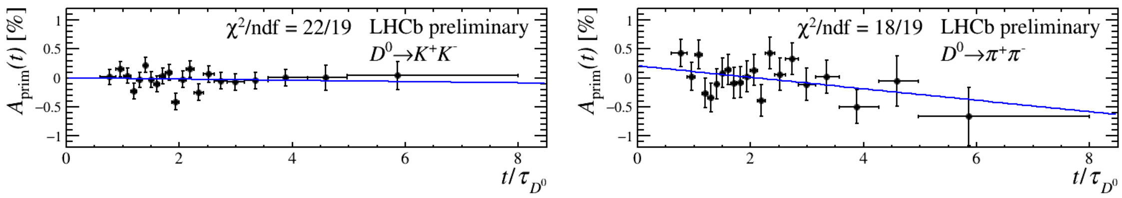

Figure 7: Fitted time-dependent asymmetry for $D^0 \to K^+K^-$ decays (left) and $D^0 \to \pi^+\pi^-$ decays (right).

The fits to the time-dependent asymmetries for both the K^+K^- and $\pi^+\pi^-$ channels is shown in Figure 7. The measured vales of A_Γ are:

$$\begin{aligned} A_\Gamma(D^0 \to K^+K^-) &= (1.3 \pm 3.5 \pm 0.7) \times 10^{-4} \\ A_\Gamma(D^0 \to \pi^+\pi^-) &= (11.3 \pm 6.9 \pm 0.8) \times 10^{-4}, \end{aligned} \tag{5.3}$$

where the uncertainties are statistical and systematic respectively. The combination of the two results and with results from previous LHCb measurements [18] is:

$$A_\Gamma = (0.9 \pm 2.1 \pm 0.7) \times 10^{-4}. \tag{5.4}$$

The result is compatible with the no *CP* violation hypothesis and dominates the world average.

6. Conclusion

The LHCb experiment has provided the most precise measurements of *CP* violation and mixing in the charm sector to date. These results include: the first observation of *CP* violation in charm, the first evidence of the mass difference between neutral charm eigenstates and measurements of *CP* asymmetries in two-body charm decays. The LHCb Upgrade I [19] and II [20] will be essential to test SM predictions of *CP* violation in charm. The measurement of the mixing parameters using $D^0 \to K_s^0\pi^+\pi^-$ decays presented in Section 3 will also benefit from the increased statistics taken during the Run 2 data taking period. New measurements of the strong phase differences from BESIII will reduce the systematic uncertainty on the mixing parameters to below the statistical uncertainty.

PoS(LHCP2019)203

References

[1] Nicola Cabibbo. Unitary symmetry and leptonic decays. *Phys. Rev. Lett.*, 10:531–533, 1963.

[2] J. H. Christenson, J. W. Cronin, V. L. Fitch, and R. Turlay. Evidence for the 2π decay of the K_2^0 Meson. *Phys. Rev. Lett.*, 13:138–140, 1964.

[3] B. Aubert et al. Observation of *CP* violation in the B^0 meson system. *Phys. Rev. Lett.*, 87:091801, 2001.

[4] R. Aaij et al. Observation of *CP* violation in charm decays. *Phys. Rev. Lett.*, 122:211803, 2019.

[5] Yuval Grossman, Alexander L. Kagan, and Yosef Nir. New physics and *CP* violation in singly Cabibbo suppressed *D* decays. *Phys. Rev. D*, 75:036008, 2007.

[6] The LHCb Collaboration. The LHCb detector at the LHC. *Journal of Instrumentation*, 3(08):S08005–S08005, 2008.

[7] R. Aaij et al. Prompt charm production in *pp* collisions at $\sqrt{s}=7$ TeV. *Nucl. Phys.*, B871:1, 2013.

[8] R. Aaij et al. Measurements of prompt charm production cross-sections in *pp* collisions at $\sqrt{s}=13$ TeV. *JHEP*, 03:159, 2016.

[9] R. Aaij, S. Benson, M. De Cian, A. Dziurda, C. Fitzpatrick, E. Govorkova, O. Lupton, R. Matev, S. Neubert, A. Pearce, H. Schreiner, S. Stahl, and M. Vesterinen. A comprehensive real-time analysis model at the LHCb experiment. *Journal of Instrumentation*, 14(04), 2019.

[10] N. L. Johnson. Systems of frequency curves generated by methods of translation. *Biometrika*, 36(1-2), 1949.

[11] R. Aaij et al. Measurement of *CP* asymmetry in $D^0 \to K^+K^-$ and $D^0 \to \pi^+\pi^-$ decays. *JHEP*, 07:041, 2014.

[12] R. Aaij et al. Measurement of the difference of time-integrated *CP* asymmetries in $D^0 \to K^+K^-$ and $D^0 \to \pi^+\pi^-$ decays. *Phys. Rev. Lett.*, 116:191601, 2016.

[13] A. Di Canto, J. Garra Ticó, T. Gershon, N. Jurik, M. Martinelli, T. Pilař, S. Stahl, and D. Tonelli. Novel method for measuring charm-mixing parameters using multibody decays. *Phys. Rev. D*, 99:012007, 2019.

[14] R. Aaij et al. Search for *CP* violation in $D_s^+ \to K_S^0\pi^+$, $D^+ \to K_S^0K^+$ and $D^+ \to \phi\pi^+$ decays. *Phys. Rev. Lett.*, 122:191803, 2019.

[15] R. Aaij et al. Search for *CP* violation in $D^+ \to \phi\pi^+$ and $D_s^+ \to K_S^0\pi^+$ decays. *JHEP*, 06:112, 2013.

[16] R. Aaij et al. Search for *CP* violation in $D^0 \to K^+K^-$ and $D^0 \to \pi^+\pi^-$ decays. *JHEP*, 10:025, 2014.

[17] The LHCb Collaboration. Search for time-dependent *CP* violation in $D^0 \to K^+K^-$ and $D^0 \to \pi^+\pi^-$ decays. 2019.

[18] R. Aaij et al. Measurement of the *CP* violation parameter A_Γ in $D^0 \to K^+K^-$ and $D^0 \to \pi^+\pi^-$. *Phys. Rev. Lett.*, 118:261803, 2017.

[19] Framework TDR for the LHCb Upgrade: Technical Design Report. (CERN-LHCC-2012-007), 2012.

[20] Physics case for an LHCb Upgrade II — Opportunities in flavour physics, and beyond, in the HL-LHC era. (CERN-LHCC-2018-027 LHCb-PUB-2018-009), 2018.

PoS(LHCP2019)203